International Journal of Scientific & Engineering Research Volume 12, Issue 9, September-2021
ISSN 2229-5518

Random Field Characterization of a Mangrove Site with CPT Data

Temple Njoku, Samuel Ejezie, Dennis Eme

Abstract— Geotechnical site characterization requires the determination of site-specific field parameters which are known to exhibit pronounced variability. The study performed a probability-based characterization of mangrove site in onshore Niger Delta region of Nigeria relying on in-situ test data from the site investigation report, with the aim of understanding the nature of spatial variability of soil properties in the soil formations. The site characterization involves the application of random field theory in estimating the three key statistical quantities that fully describe spatial variability of a soil property (mean μ, variance σ^2, and correlation structure θ), using data from select 16 CPT holes. The estimation of the correlation structure, which defines the distance over which the value of the soil property remains similar in the field, was performed by fitting correlation theoretical models to the experimental correlation functions in the vertical and horizontal directions. The vertical correlation lengths of cone tip resistance in the clay layers fall within the range 0.135-0.250m with the coefficient of variation (COV) decreasing as the depth of occurrence of the clay layer increases. The site is generally isotropic as the horizontal correlation lengths of the soil parameters did not show any directional dependency, being similar in all directions with the correlation length of the cone tip resistance in the eastings and northings ranging from 0.85 to a maximum of 3.18. This information is useful in deciding on the need for additional site investigation with closely spaced CP test holes and sampling depths.

Index Terms—Coefficient of variation, correlation length, Random field theory, Site characterization, spatial variability.

1 Introduction

SOIL formation is a continuous natural process and as a result its properties present spatial structure both vertically and horizontally, with a higher tendency for similar values at points close to each other than at points far apart [1], [2]. The conventional tool used in practice to account for spatial variability is factor of safety in which a recommended value reflects the engineer's confidence in the available data, and experience. More recent research efforts, however, apply the hypothesis of randomness in resolving issues of variability as characterization of spatial variability of soil properties is readily performed using statistical and probabilistic methods [3]. These methods have evolved from simple statistical description of the soil property to the more intricate random field theory.

The study carried out a probability-based characterization of a mangrove swamp site in Niger Delta region of Nigeria using in-situ data from the site investigation report. The cone tip resistance data from select 16 CPT were analyzed and modeled using the random field theory culminating in the geotechnical characterization of the site

2 Random field theory

2.1 Spatial Variability of Soil Property

The patterns of spatial variability in soil parameters might be discrete or continuous [4]. The soil property exhibits continuous spatial variability when it varies continually from one site to another throughout the soil unit and is characterized by a steady fluctuation around an average trend of variation. Discrete spatial variability occurs in soil units that exhibit continuous spatial variability but with a mixture of dislocations such as faults, lenses, or fills arising from their geological and morphological history. Notwithstanding the pattern of the spatial variability, the characterization of a site using the random field model assumes that every point in the field is a random variable and the soil properties are spatially dependent, with such dependence decreasing as the separation distance of the points increases.

A full characterization of spatial variability of a soil property requires the description of the soil property in terms of three statistical quantities of mean, variance, and scale of fluctuation or correlation length which gives an indication of the distances within which material property values exhibit a considerable correlation [5]. Every point in a random field is a realization and the statistical parameters describing the field are determined from only one realization making it imperative that the random field should locally satisfy certain ergodicity conditions [4]. One of such conditions is that of stationarity (or homogeneity) of data which allows the complete joint distribution to be quantified by the mean vector and covariance matrix and makes the distribution independent on spatial position but dependent only on relative positions of points. A random field of non-stationary mean and variance can always be linearly transformed into a weak stationary field using Equation (1) [6].

$$X'(t) = [X(t)-\mu(t)]/\sigma(t) \quad (1)$$

With transformation, the random field $X'(t)$ will have a mean of zero and unit variance throughout the given domain. Generally, a transformation of the variables is often carried out by

---

- *Temple Njoku is currently pursuing PhD degree program in geotechnical engineering at the University of Port Harcourt, Nigeria, +2348066402293. E-mail: templenjoku@gmail.com*
- *Samuel Ejezie is a professor of civil engineering and currently Head of Department of Civil engineering, Federal University Otuoke Bayelsa State Nigeria, +2348034701399. E-mail: samejezie@yahoo.co.uk.*
- *Dennis Eme is the acting Director, Centre for Geotechnical and coastal engineering research and lecturer at Department of Civil and Environmental Engineerin, University of Port harcourt, Nigeria, +2348055943566. E-mail: dennis.eme@uniport.edu.ng*

decomposition which converts the non-stationary field to stationary or nearly stationary field, simplifying the application of the random field theory. The decomposition transformation technique breaks down the soil property into deterministic trend component and a set of residuals fluctuating about the trend. Considering a one-dimensional case in the depth (z) coordinate, the decomposition can be expressed in form of an additive equation [2], [8]:

$$\Psi(z) = t(z)+\xi(z) \tag{2}$$

The decomposition procedure is primarily aimed at obtaining an estimate and removing the deterministic component, t(z), while ensuring that the residual random component, ξ(z), remains stationary. The residual component is then modeled by means of statistical analysis to fully characterize the spatial variability of the soil parameter. The scale of fluctuation, θ, and the autocovariance function, C(τ) defines the spatial structure of the residual component, where τ is the distance between observation points [9].

Developing a model for the spatial variability of geotechnical material requires at least three statistical parameters: the mean, μ; a measure of variance, σ^2 (standard deviation σ, or coefficient of variation); and a scale of fluctuation, θ, which links the correlation of the geotechnical properties with distance [15]. A high value θ indicates that the property varies slowly with distance from the mean, indicating a more continuous deposit, whereas a low value indicates that the property fluctuates rapidly around the mean, indicating a more randomly variable material [10].

Two important statistical properties of the random field in modeling the spatial variability of the soil property are the autocovariance, c_k, and autocorrelation coefficient, ρ_k, at lag k. These two properties are usually estimated from the samples obtained from a population. The sample autocovariance c_k^* and the sample autocorrelation coefficient, at lag k, r_k, are defined as follows [10]:

$$c_k^* = \frac{1}{n}\sum_{i=1}^{n-k}(X_i - \bar{X})(X_{i+k} - \bar{X}) \tag{3}$$

and

$$r_k = \frac{c_k^*}{c_0} = \frac{\sum_{i=1}^{n-k}(X_i-\bar{X})(X_{i+k}-\bar{X})}{\sum_{i=1}^{n}(X_i-\bar{X})^2} \tag{4}$$

$\bar{X}$ = average of the observations $X_1, X_2, \ldots, X_n,\ and\ 0 \le k \le n$

The plot or graph of c_k^* for lags $k = 0,1,2,\ldots$ represents the sample autocovariance function (ACVF), or auto-variogram while the plot of r_k for lags $k = 0,1,2,\ldots K$ represents the sample autocorrelation (ACF), where K is the maximum number of lags for r_k calculations (e.g., $K = n/4$). Estimates for scale of fluctuation are usually obtained by fitting the theoretical correlation model (Table I) to the sample autocorrelation function [7], [9], and [11].

The correlation length is the lag number when $\rho_k = 0$ and this is defined by the Bartlett's limit - Equation (5) [12], [13].

$$r_k = \frac{c_k^*}{c_0} = \frac{\sum_{i=1}^{n-k}(X_i-\bar{X})(X_{i+k}-\bar{X})}{\sum_{i=1}^{n}(X_i-\bar{X})^2} \tag{5}$$

For two locations separated by horizontal and vertical distances Δh and Δz respectively, in a three-dimensional zero-mean random field ξ(x,y,z), the autocorrelation can be estimated with Equation (6), where ξ is the residual or detrended property field and (x,y,z) is the spatial location, with x and y being the horizontal coordinates and z the depth coordinate [14].

$$\rho(\Delta h, \Delta z) = \frac{Cov[\xi(x,y,z),\xi(x+\Delta x,y+\Delta y,z+\Delta z)]}{\sqrt{Var[\xi(x,y,z)]}\times\sqrt{Var[\xi(x+\Delta x,y+\Delta y,Z+\Delta z)]}} \tag{6}$$

where var(.) denotes variance: cov(..) denotes covariance, $\Delta h=(\Delta x^2+\Delta y^2)^{0.5}$ is the horizontal separation distance.

2.2 Scale of Fluctuation

The scale of fluctuation, θ , is a measure of the distance within which points in a domain are significantly correlated and it conveniently describes the spatial variability of a soil property [15]. The correlation between two points depends on how the separation distance compares with θ. Given the importance of θ in the spatial variability description of soil property in a random field, extensive research work aimed at developing more rational approaches in determining accurate estimates of the scale of fluctuation have been carried out [16], [17], [18], [19]. Small values of θ obtained from any of the models indicate that the correlation function decays rapidly to zero with increasing τ (meaning that the correlation between the two points under consideration are rapidly smaller) resulting in a rougher random field. As $\theta \to 0$, all points within the domain become uncorrelated and the field becomes extremely rough. Conversely, increasing values of θ is an indication that the property field is smoother meaning that the field is showing less variability converging to a uniform field when $\theta \to \infty$ [20]. In practice, estimation of θ is done by fitting the theoretical correlation to the experimental correlation function [7], [9], [11].

Table I: Some common correlation models, Source: [20]

Correlation Model	Expression	Scale of Fluctuation
Simple exponential	$\rho(\tau) = \exp[-\lvert\tau\rvert/b]$	2b
Gaussian exponential	$\rho(\tau) = \exp\{-\pi[\lvert\tau\rvert/c]^2\}$	$\sqrt{\pi}c$
Second-order auto-regressive process	$\rho(\tau) = \exp^{-\lvert\tau\rvert/d}\{1+(\lvert\tau\rvert/d)\}$	4d
Cosine exponential	$\rho(\tau) = \exp^{-\lvert\tau\rvert/\rho}\cos(\tau/\alpha)$	α

International Journal of Scientific & Engineering Research Volume 12, Issue 9, September-2021
ISSN 2229-5518

3 Methodology

3.1 Study Area and Data Acquisition

The area of study falls within the Tertiary Niger Delta which occurs at the southern end of Nigeria bordering the Atlantic Ocean and extends from about longitudes 30-90E and latitude 40 30′-50 20′N.

The study used data from a geotechnical site investigation report of a refinery project with a total of 96 data sets available, out of which 20 (16 CPT and 4 borehole data), were carefully selected for the study to present an equally spaced CPT grid, suited for random field theory application. A summary of the data set is presented in Table II

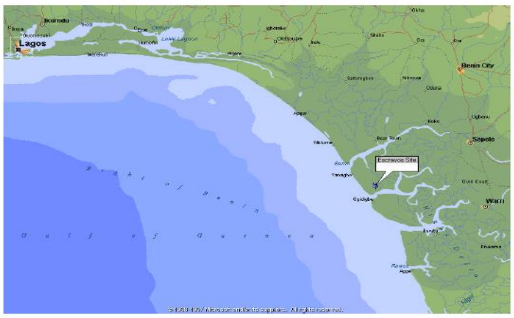

Figure 1. Location of study area

Table II. Study data set

Data		Refinery		
	CP 10	CP 14	CP 19	CP 24
CPT	CP11	CP16	CP20	CP26
	CP12	CP17	CP22	CP27
	CP13	CP18	CP23	CP28
Borehole	BH8	BH9	BH10	BH11

3.2 Method of Data Analysis

The method of data analysis followed the same steps of an accompanying paper [23]. The soil profile generated from the borehole log and CPT data identified five distinct soil layers and analyses were performed for each of the soil layers. To ensure statistical homogeneity or stationarity within the domain for a seamless application of the random field theory, the entire soil profile within the zone of influence was divided into number of statistically homogeneous or stationary sections, and the data within each layer subjected separately to statistical analysis [21].

Data from each CPT test hole was evaluated to determine the value of geotechnical parameter at the different strata of the soil profile. The examination of data of each CPT to determine the value of the realization at any strata was carried out using the following steps [10]:

- Examine the data of the parameter across the depth and transform the non-stationary data into stationary data. Where the data exhibited a trend, decomposition was required otherwise linear transformation into a weak stationary field was performed.
- Decomposition involved separating the trended data into a slowly changing trend component and a random or residual component. The ordinary least square (OLS) method was used to estimate the trend.
- To ensure stationarity of the residuals, eyeballing and the Kendal's τ test was used to examine for stationarity. With stationarity confirmed, it was assumed that the residuals are normally distributed.
- Calculate the sample autocovariance and autocorrelation functions using Equations (3) and (4) respectively.
- Estimate the correlation length, θ, by fitting a theoretical model from Table 1 to the plot of sample ACF over lag distance
- Calculate the Bartletts distance (i.e., distance over which the samples are autocorrelated).

The vertical spatial variability was analyzed by estimating the correlation distance within each soil layer for the cone tip resistance (Equation (4)) while the horizontal spatial variability was analyzed by fitting a theoretical model to the sample autocorrelation function (ACF) of pairs of CP test holes (Equation (6)). Given the wide spacing between the CP test holes, three additional intermediary test holes were generated using data from pair of field CP profiles which effectively reduced the spacing between test holes from 50m to 12.5m. The 2-dimensional spatial variability was estimated in two horizontal directions (northing and easting).

4 Results and Discussion

4.1 Random Field Characterization – vertical spatial variability

The random field modeling for vertical variability of q_c is illustrated using data from the CP26 test hole. The plot of q_c against depth from the CPT interpretation software is shown in Figure 2. Each stratum was examined for spatial trend and where trends existed it was removed using Ordinary Least Square (OLS) method.

The data exhibited both linear and quadratic trends. Figure 3 shows a trend model with residual over the depth band shown in Figure 4. The clay soil layers followed a linear trend while the sand and gravelly layers followed a quadratic trend. For the strata lying within 12.5-25m depth, the residual, r_{oc} is obtained by subtracting the trend value from the measured value as in equation (7).

$$r_{oc} = q_c - (9.3999 - 7.203x + 1.9175x^2 - 0.0951x^3) \quad (7)$$

Results of the Kendall's τ test had all the soil layers τ values within the range ± 1 and closer to 0 indicating stationarity of data. To estimate the correlation length, the autocorrelation functions (ACF) were computed for separation distances $\tau_k = k\Delta z$ for lags $k = 0,1,2,\ldots n/4$ where $\Delta z = 0.25m$ (i.e., sampling interval) and n=number of data points within layer. The plot of sample ACF over the separation distances with the cosine exponential theoretical model superimposed, for soil layer at 16.5-37.5m depth is shown in Figure 5.

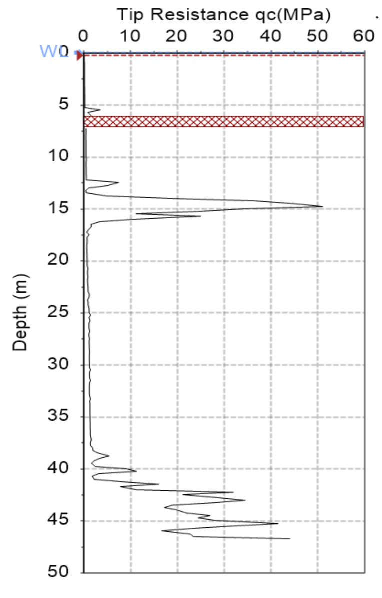

Figure 2: Cone tip resistance plot of CP26

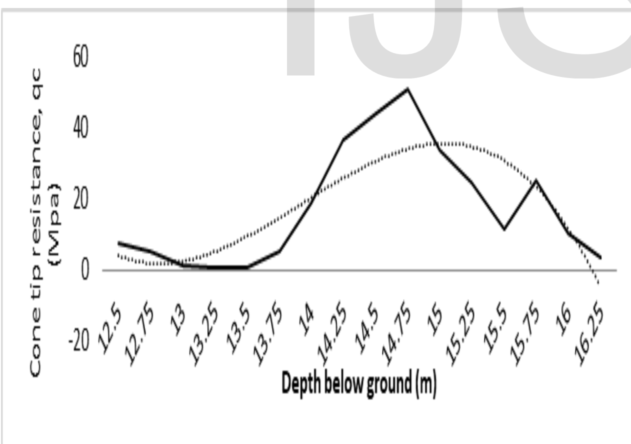

Figure 3: Measured cone tip resistance with quadratic trend for at 12.5-16.25m depth

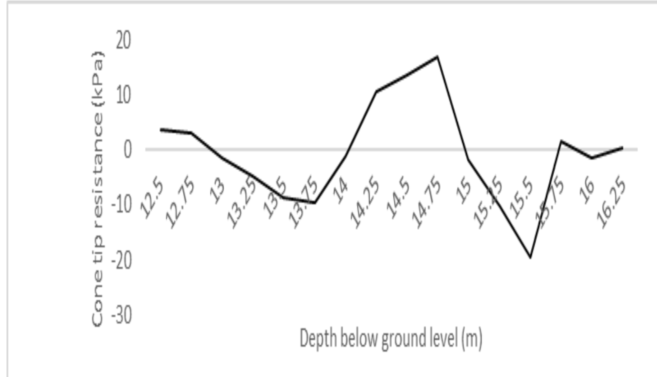

Figure 4: Residuals of qc, after trend removal at 12.5-25m depth

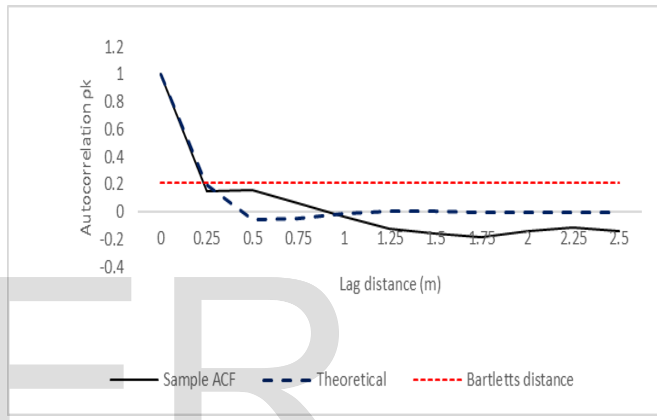

Figure 5: Sample and model ACF from residual of q_c at 16.5-37.5m depth

Summary of results of vertical variability analyses of CP26 test hole is presented in Table IV. Similar analyses were repeated on the data from each of the other 15 CP test holes and the estimated vertical scale of fluctuations are presented in Table V for the clay soil units and Table VI for the sand and gravelly soil units.

Table IV: Summary of results of vertical variability analyses on CP26 test hole data

Depth range of stratum (m)	**Value of Parameter (m)**	**Bartlett's distance**	**Scale of Fluctuation, θ(m)**
0.25-5.25	α=0.478	±0.428	0.250
6.25-12.25	α=0.105	±0.392	0.135
12.5-16.25	α=0.345	±0.490	0.248
16.5-37.5	α=0.182	±0.216	0.176
37.75-46.5	α=0.261	±0.490	0.128

Table V: Vertical Scale of Fluctuation, θ_v, of cone tip resistance, q_c, in clay units

Sensitive fines	0.25 - 5.25m		
Clay		6.25 – 12.25m	16.5 – 37.5m
Variable	θv(m)	θv(m)	θv(m)
CP10	0.246	0.162	0.186
CP11	0.195	0.173	0.212
CP12	0.184	0.168	0.179
CP13	0.224	0.161	0.210
CP14	0.246	0.165	0.202
CP16	0.214	0.142	0.180
CP17	0.238	0.158	0.204
CP18	0.147	0.154	0.199
CP19	0.210	0.145	0.201
CP20	0.167	0.172	0.212
CP22	0.247	0.174	0.216
CP23	0.195	0.165	0.183
CP24	0.246	0.175	0.188
CP26	0.250	0.135	0.176
CP27	0.135	0.188	0.216
CP28	0.165	0.167	0.181
Mean (m)	0.207	0.163	0.197
Std Dev (m)	0.038	0.014	0.014
COV (%)	18.6	8.4	7.4

Table VI: Vertical Scale of Fluctuation of cone tip resistance in sand and gravelly units

Sand	12.5 – 16.25m	
Gravely Sand		37.75 - 46.5m
Variable	θv(m)	θv(m)
CP10	0.265	0.182
CP11	0.237	0.198
CP12	0.321	0.180
CP13	0.237	0.210
CP14	0.246	0.200
CP16	0.231	0.242
CP17	0.322	0.183
CP18	0.280	0.203
CP19	0.280	0.225
CP20	0.288	0.220
CP22	0.313	0.250
CP23	0.284	0.240
CP24	0.249	0.254
CP26	0.248	0.128
CP27	0.135	0.125
CP28	0.268	0.220
Mean (m)	0.262	0.204
Std Dev (m)	0.045	0.038
COV (%)	17.2	18.8

4.2 Random Field Characterization – horizontal spatial variability

The determination of the correlation structure in the horizontal direction is illustrated using the residuals of CPT data of CP 26 and CP27 for the easting and CP20 and CP26 for the northing. The sample correlation functions were determined for each layer in the soil profile. The plots of the sample ACF over the lag distance (at 1m intervals) are shown in Figures 6, 7, 8, 9 and 10. Theoretical models were fitted to estimate the scale of fluctuation with the simple exponential model providing the closest fit to the sample ACF. Table VII provides a summary of the results. The summary of analyses carried out between other pairs of CPT hole across the study field in the easting and northing directions are presented in Tables VIII and IX respectively.

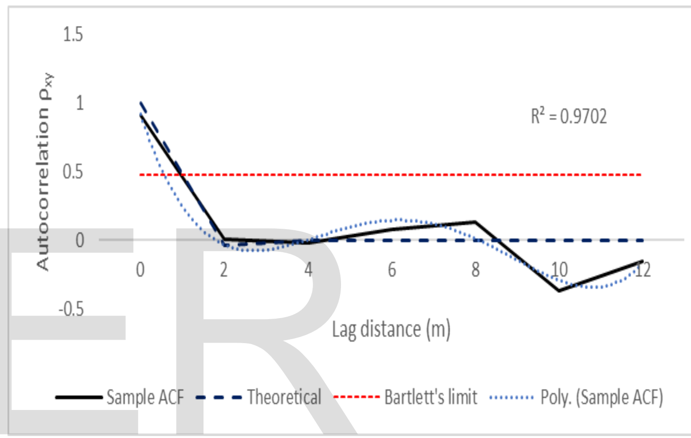

Figure 6: ACF of CP26 & CP27 @ 0 - 5.25m depth

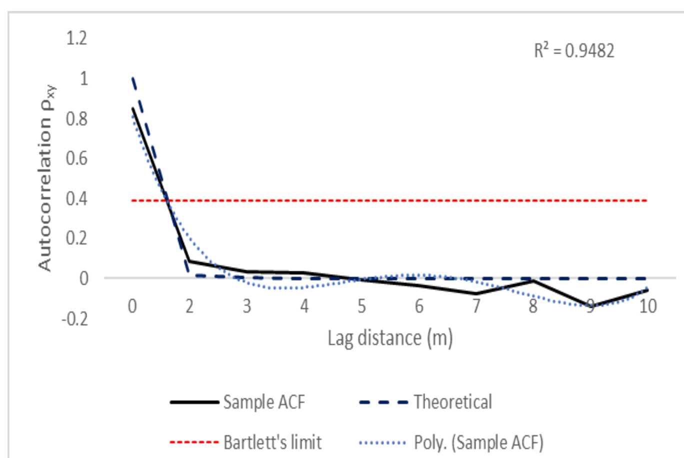

Figure 7: ACF of CP26 & CP27 @ 6.25 – 12.25m depth

ISSN 2229-5518

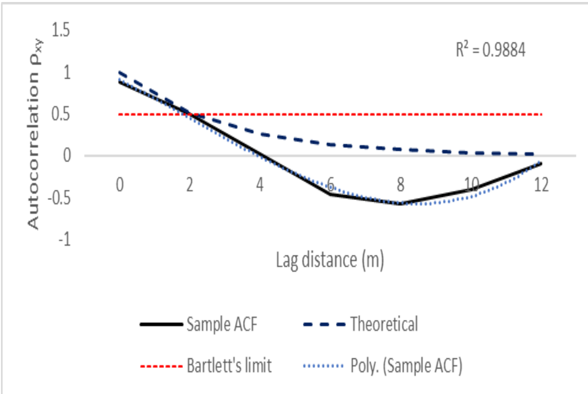

Figure 8 ACF of CP26 & CP27 @ 12.25 - 16.00m depth

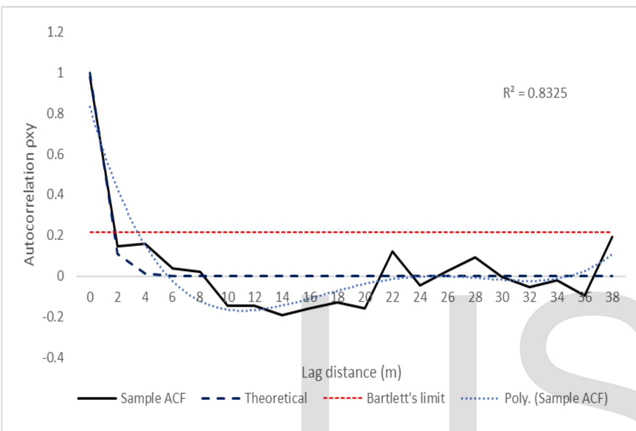

Figure 9: ACF of CP26 & CP 27 @ 16.25 - 37.5m depth

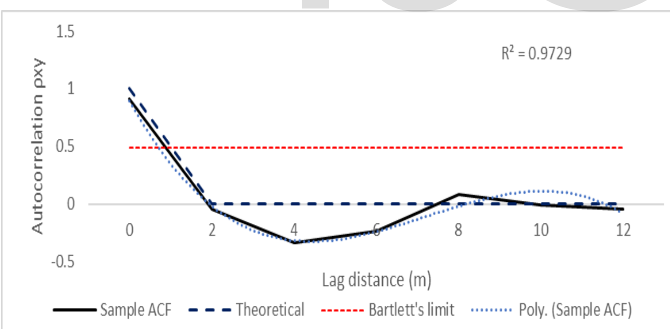

Figure 10: ACF of CP26 & CP27 @ 37.75 - 41.5m depth

Table VII: Summary of results of horizontal variability analyses

Depth range of stratum (m)	Value of Parameter (m)	Bartlett's Limit (m)	Scale of Fluctuation, θ_H (m)
0.25-5.25	α=0.700	0.428	0.987
6.25-12.25	α=0.500	0.392	1.200
12.5-16.00	α=1.200	0.490	2.200
16.25-37.5	α=0.900	0.216	1.800
37.75-41.5	α=0.400	0.490	1.000

Table VIII: Horizontal variability analyses of qc -Easting

Avg. thickness	0.25 - 5.25m	6.25 – 12.25m	12.5 – 16.0m	16.5 – 37.5m	37.75 – 46.5m
Variable	θ_H(m)	θ_H(m)	θ_H(m)	θ_H(m)	θ_H(m)
CP10 –11	2.000	1.900	2.300	2.800	0.900
CP11 – 12	1.500	1.500	2.400	2.800	1.00
CP12 –13	0.850	1.300	2.200	2.100	1.200
CP14 –16	1.900	1.400	2.700	2.500	0.900
CP16 –17	2.200	1.200	2.400	1.800	1.200
CP17 – 18	2.000	1.400	2.600	1.900	1.200
CP19 –20	1.500	2.100	2.500	2.700	1.100
CP20 – 22	2.300	1.400	2.400	2.600	1.400
CP22 –23	1.650	1.300	2.200	2.000	1.400
CP24-26	2.400	1.700	1.800	2.300	1.000
CP26 – 27	0.987	1.200	2.200	1.800	1.000
CP27 –28	1.500	1.400	2.300	2.500	1.100
Mean (m)	1.732	1.483	2.333	2.317	1.117
Std Dev m)	0.492	0.279	0.230	0.383	0.170
COV (%)	28.4	18.8	9.9	16.5	15.2

Table IX: Horizontal variability analyses of qc - Northing

Avg. thickness	**0.25 - 5.25m**	**6.25 – 12.25m**	**2.5 – 16.0m**	**16.5 – 37.5m**	**37.75 – 46.5m**
Variable	θ_H(m)	θ_H(m)	θ_H(m)	θ_H(m)	θ_H(m)
CP10 – 14	2.050	0.870	1.700	1.670	0.980
CP11 – 16	1.920	1.130	1.570	1.280	1.020
CP12 – 17	2.820	1.070	1.650	1.660	0.950
CP13 – 18	3.180	0.850	1.850	1.475	1.050
CP14 – 19	1.650	0.980	1.570	1.670	0.990
CP16 – 20	3.010	1.100	2.120	1.525	1.010
CP17 –22	2.520	1.150	1.560	1.650	0.950
CP18 – 23	2.900	0.880	1.670	1.650	0.980
CP19 – 24	2.100	1.010	2.260	1.550	0.960
CP20-26	2.800	1.200	2.500	1.500	1.000
CP22 –27	3.050	1.600	2.120	1.750	0.970
CP23 –28	2.200	1.120	2.450	1.700	0.950
Mean (m)	2.167	1.080	1.918	1.590	0.984
Std Dev (m)	0.512	0.201	0.354	0.130	0.031
COV (%)	20.4	18.6	18.4	8.2	3.2

The correlation lengths of the cone tip resistance exhibited similar characteristics in the vertical and horizontal directions within clay deposits with no marked behavioral pattern observed in sand deposits. Within the clay units, the coefficient of variation of the correlation length of the geotechnical parameter decreased as depth increased (Table X, and XII), suggesting that variability in the clay soils depends on the location depth of the deposit. The deeper the deposit the less variable is the soil property, an indication of the stable state of the deposit at such depths which is largely attributed to the effect of in-situ confining stresses. With larger confining stress in soils, void ratio reduces over time resulting in consolidation of clay deposits hence the stable state and associated low coefficient of variation. The upper clay layers exhibited more variability than deep lying layers of the same soil group due to the increased void ratio. Conversely, the coefficient of variation in the sand deposits did not display consistent behavioral pattern as observed in clay (XI and XIII) with the trend varying from one orientation to the other. It increased with depth in easting and decreased with depth in the northing.

The estimated scale of fluctuation defines the distance over which the soil parameter is correlated, implying that if the value of the parameter is large at a point, it is expected to remain large over the correlation distance. Beyond the distance defined by the Bartlett's limit, the value of the parameter is expected to be different. Thus, the cone tip resistance in the upper clay deposit is correlated over a length of 0.135-0.250m in the vertical direction as shown in Table X. The minimum and maximum estimated correlation lengths of the parameter in the soil groups encountered are shown in Tables X-XIII. Furthermore, the correlation length or scale of fluctuation in the horizontal coordinates (easting and northing directions) are similar, an indication of an isotropic field.

Table X: Variation of scale of fluctuation with depth in clay in the vertical direction

Depth range (m)	Vertical scale of fluctuation θ_V range (m)		
	Cone tip resistance, q_c		
	min	max	COV%
0.25-5.25	0.135	0.250	18.6
6.25-12.25	0.135	0.188	8.4
16.50-37.50	0.176	0.216	7.4

Table XI: Variation of scale of fluctuation with depth in sand in the vertical direction

Depth range (m)	Vertical scale of fluctuation θ_V range (m)		
	Cone tip resistance, q_c		
	min	max	COV%
12.5-5.25	0.135	0.322	17.2
37.75-46.50	0.125	0.254	18.8

Table XII: Variation of scale of fluctuation of qc with depth in clay in the horizontal direction

Depth range (m)	Horizontal scale of fluctuation θ_h range (m)					
	Cone tip resistance, q_c (Easting)			Cone tip resistance, q_c (Northing)		
	min	max	COV%	min	max	COV%
0.25-5.25	0.850	2.400	28.4	1.650	3.180	20.4
6.25-12.25	1.200	2.100	18.8	0.850	1.600	18.6
16.50-37.50	1.800	2.800	16.5	1.280	1.750	8.2

Table XIII: Variation of scale of fluctuation of q_c with depth in sand in the horizontal direction

Depth range (m)	Horizontal scale of fluctuation θ_h range (m)					
	Cone tip resistance, q_c (Easting)			Cone tip resistance, q_c (Northing)		
	min	max	COV%	min	max	COV%
12.5-16.00	1.800	2.700	9.9	1.560	2.500	18.4
37.75-46.50	0.900	1.400	15.2	0.950	1.050	3.2

5 CONCLUSIONS

The generalized soil profile comprises of upper soft organic sensitive fines and alternating layers of clay and sand/gravely sand. The upper organic sensitive fines exhibit small correlation length for the cone tip resistance, ranging from 135mm to 250mm, indicative of a rough field up to a depth of about 5m. This implies that the geotechnical properties on this layer are largely unpredictable and changes over extremely small distances. In practice, such soil is adjudged unsuitable to support a foundation and will be recommended for replacement or preloading.

The coefficient of variation of the correlation length of the soil parameter decreases as depth increases indicating that the soil properties are more predictable at deep lying strata, especially for clay soils. The upper lying clay soils exhibit more variability than the deeper lying clay units. This phenomenon is attributed to the effect of in-situ confining stresses on the soil layer which acts to reduce the void ratio and increase the consolidation of the clay units at such depths.

The random field analyses show that the site is generally isotropic as the correlation lengths of the soil parameters were similar along different directions (eastings and northings). The cone tip resistance range of correlation length in the easting and northing directions are 0.85-2.8 and 0.85-3.18 respectively. With this information, it is possible to decide if additional site investigation with closely spaced CP test holes and sampling depths will be required.

REFERENCES

[1] Nadim, F. (2015), "Accounting for uncertainty and variability in geotechnical characterization of offshore sites" *Geotech Safety and Risk* V 23, T. Schweckendiek et al. (Eds) https://doi.org/10.3233/978-1-61499-580-7-23

[2] Chakraborty, R, and Dey, A., (2018), "Stochastic modeling of the spatial variability of soil" *Advances in Numerical Methods in Geotechnical Engineering* H. Shehata and C. S. Desai (Eds.): GeoMEast 2018, 144–155, 2019. https://doi.org/10.1007/978-3-030-01926-6_11

[3] Onyejekwe, S., (2012). "Characterization of soil variability for reliability-based design" *Doctoral Dissertation*. 2142. https://scholarsmine.mst.edu/doctoral_dissertations/2142

[4] Baker, J. and Calle, E. (2006). Section 3.7: Soil Properties, *JCSS Probabilistic Model Code*,

[5] Vanmarcke. E.H. (1977). "Probabilistic modeling of soil profiles". *Journal of the Geotechnical Engineering Division*. ASCE. l03(GTll): 1227-1245.

[6] Fenton, G., and Griffiths, D.V., (2008). *Risk Assessment in Geotechnical Engineering*, John Wiley & sons, New Jersey.

[7] Uzielli, M., Lacasse, S., Nadim, F., and Phoon, K.K. (2006), "Soil variability analysis for geotechnical practice" *Proc. of the 2nd International Workshop on Characterization and Engineering Properties of Natural Soils, Singapore*, 3: 1653-1752 https://www.researchgate.net/publication/266136333

[8] Baecher, G.B. & Christian, J.T. (2003). *Reliability and statistics in geotechnical engineering,* John Wiley & Sons, New York

[9] Oguz, E. A., and Huvaj, N. (2019). "Spatial probabilistic evaluation of offshore/nearshore sea bottom soils based on cone penetration tests", *Bulletin of Engineering Geology, and the Environment*, https://doi.org/10.1007/s10064-019-01608-w

[10] Jaksa, M.B. (2006). "Modeling the natural variability of an over-consolidated clay in Adelaide, South Australia". in T.S. Tan, K.K. Phoon, D.W. Hight & S. Leroueil (eds.), *Proceedings of the 2nd International Workshop on Characterization and Engineering Properties of Natural Soils*. Singapore, November 29 – December 1, 2006. The Netherlands: Taylor & Francis.

[11] Zhu, H and Zhang, I.M., (2013) "Characterizing geotechnical anisotropic spatial variations using random field theory", *Canadian Geotech. J.* 50: 723-734, https://dx.doi.org/10.1139/cgj-2012-0345

[12] Box, G. E. P. and Jenkins, G. M. (1970). *Time Series Analysis: Forecasting and Control*, Holden-Day, San Francisco, 553 p.

[13] Chatfield, C. (1975). *The Analysis of Time Series: Theory and Practice*, Chapman and Hall, London, 263 p

[14] Ching, J., Wu T., Stuedlein, A. W., and Bong, T., (2017) Estimating horizontal scale of fluctuation with limited CPT soundings, *Geoscience Frontiers*, 1-12. https://doi.org/10.1016/j.gsf.2017.11.008

[15] Vanmarcke, E.H., (1983). *Random fields: analysis and synthesis*. MIT Press, Cambridge, Mass.

[16] Fenton, G. A., and Griffiths, D.V., (2005). "Three-dimensional probabilistic foundation settlement", *ASCE Journal of Geotechnical and Geoenvironmental engineering.* 131 (2), 232-239

[17] Griffiths, D.V., Huang J.S. and Fenton, G.A., (2009), Influence of spatial variability on slope reliability using 2-D random fields, ASCE Journal of Geotechnical and Geoenvironmental engineering. 135 (10), 1367-1378

[18] Hicks, M.A. and Spencer, W. A., (2010). " Influence of heterogeneity on the reliability and failure of a long 3D slope". *Computers and Geotechnics*, 37 (7-8), 948-955.

[19] Cassidy, M.J., Uzielli, M. and Tian, Y., (2013). "Probabilistic combined loading failure envelopes of a strip footing on spatially variable soil'. *Computers and Geotechnics,* 49, 191-205.

[20] Lloret-Cabot, M., Fenton, G.A., and Hicks, M.A. (2013). "On estimation of scale of fluctuation in geostatistics", *Georisk: Assessment and Management of Risk for Engineered Systems and Geohazards*, 8:2, 129-148 https://doi.org/10.1080/17499518.2013.871189

[21] NovoCPT®, (2019) Cone Penetration Test (CPTu) processing Software, *NovoTech Software*, North Vancouver, Canada. http://www.novotechsoftware.com

[22] Phoon, K. K., Quek, S. T., An, P., (2003b). "Identification of statistically homogeneous soil layers using modified Bartlett statistics". *ASCE Journal of Geotechnical and Geoenvironmental Engineering* 129(7), 649-659 https://doi.org/10.1061/(ASCE)1090-0241(2003)129:7(649)

[23] Njoku, T., and Ejezie, S, (2021). "Predictive model of undrained shear strength based on random field theory" Paper accepted for publication by *International Journal of Scientific & Engineering Research*, September 2021.